

Ice fabric development with a new fabric evolution model

M. Hay¹, E.D. Waddington¹

¹*Department of Earth and Space Sciences, University of Washington*

ABSTRACT. Ice crystal orientation fabric has a strong influence on ice flow due to the plastic anisotropy of ice. The evolution of crystal fabric is driven by strain-induced grain rotation, as well as recrystallization. Most fabric-evolution models ignore many of the physical processes involved, or are valid only for highly parameterized fabrics. In this paper, we outline a new fabric model that treats a variety of processes affecting fabric development, and is suitable for inclusion in flow models. The model is checked against thin-section data from the WAIS divide core. In addition, the model shows that that a large proportion of the observed variability in thin section samples is likely to be effectively stochastic in nature.

INTRODUCTION

An individual ice crystal has an anisotropic creep response, deforming most easily in shear parallel to the crystal basal plane. Plastic deformation of an ice polycrystal depends on the orientations of its constituent grains (Azuma, 1994). A polycrystal that is initially isotropic will develop a lattice-preferred orientation in response to applied strain, thus causing it to have a bulk anisotropic response. The development of a preferred orientation is guided primarily by intracrystalline slip. Due to interference between grains, there is a tendency for the c-axes to rotate away from the directions of principal extensional. In addition to rotation, recrystallization affects both grain size and orientation distribution. Near the melting point, migration recrystallization allows the nucleation of new, strain-free grains. These new grains grow rapidly at the expense of older grains with high strain energy (Duval and Castelnau, 1995). Polygonization is another recrystallization process in which dislocations in a highly strained grain arrange into a subgrain boundary, eventually producing two grains as the misalignment increases (Alley and others, 1997). Although the grains typically are misaligned by only a few degrees, this does have the effect of preventing the orientation distribution function from attaining a sharp maximum.

In order to model fabric development, a homogenization scheme must be used in order to relate the macroscopic stress and strain rate experienced by the polycrystal to the state experienced by individual grains. The two possible end members are the Taylor-Bishop-Hill (homogeneous strain) (Taylor, 1938) and the Sachs (homogeneous stress) (Sachs, 1928) assumptions. For many materials such as metals with several active slip systems, homogeneous strain turns out to be a good assumption. It has the advantage of maintaining compatibility in between grains, in assuming that hard-oriented grains receive correspondingly more stress in order to produce the same strain as soft grains. For ice, in which basal dislocation glide is by far the easiest slip system, homogeneous stress is a better assumption (Thorsteinsson, 2002). The actual situation is intermediate, with softer-oriented grains receiving more strain less stress. Grain compatibility is maintained through intercrystalline slip, and shear on basal and non-basal slip systems. Molinari and others (1987) developed the viscoplastic self-consistent homogenization (VPSC) model. Each individual grain is represented as an inclusion in a homogeneous equivalent medium representative of the bulk polycrystal properties. This can allow for a compromise between the homogeneous stress and homogeneous strain assumptions. The VPSC model has been used for ice by several investigators (e.g. Gillet-Chaulet and others (2005), Castelnau and others (1997)). Azuma and Goto-Azuma (1996) used a conceptually similar scheme in which stress over the polycrystal is partitioned by the resolved shear stress on the basal plane of each individual crystal. Thorsteinsson (2002) took a different approach using the assumption of a polycrystal with cube-like topology, with each grain having six neighboring grains. The velocity gradient on an individual crystal was adjusted by a softness parameter,

$$\epsilon^c = \frac{1}{\gamma + 6\mu} \left(\gamma T_0 + \mu \sum_{i=1}^6 \frac{T_i}{T_0} \right) \quad (1)$$

where T_i is the resolved shear stress of grain i , T_0 is the resolved shear stress of the central grain, and γ and μ adjust the relative contributions of the central grain and the six nearest neighbors. This has the effect of making a soft (high resolved shear stress) grain surround by hard (low resolved shear stress) grains harder, and vice-versa.

In this paper, we outline a general fabric-evolution model, using discrete grains rather than a continuous distribution to represent the polycrystal. Each grain possesses various physical properties such as radius and accumulated strain. In addition, each grain has several neighboring grains, with which it interacts. This is somewhat similar to the approach taken by Thorsteinsson (2002) and by Kennedy and others (2013) to account for nearest-neighbor interactions. However, the previous works assumed each grain has 6 neighbors, whereas this model allows for more or fewer neighbors. Unlike previous discrete models, this model maintains mass balance in the polycrystal. Grains grow only at the expense of neighboring grains, as opposed to assuming a parabolic growth-law (e.g. Gow (1969)). Recrystallization also obeys mass balance, with the nucleated grain removing mass from its neighbors. Polygonization likewise is mass-conservative, with a grain splitting its volume in half. Increases in average grain size can occur only by the disappearance of some grains. Thus, the model has explicit connectivity

to represent spatial information. The model uses strain rate and vorticity as input rather than stress. While ice fabric evolution is physically deterministic, it depends highly on effectively unobservable properties such as dislocation density distributions, inclusions, impurity content, and other factors. Thus, it is justified to treat recrystallization as being stochastic.

GRAIN ROTATION

The most important process governing the formation of crystal fabrics is deformation-induced grain rotation. Grain rotation is described using a Jefferys-Type equation (Azuma, 1994):

$$\dot{c}_i = \zeta (W_{ij}c_j + D_{ij}c_j + c_ic_jc_kD_{jk}) \quad (2)$$

where c_i is the unit vector in the direction of the c -axis, D_{ij}^g are W_{ij}^g , respectively, are the strain rate tensor and vorticity tensor in the vicinity of the grain. ζ is the softness parameter, which allows for nearest neighbor interaction by effectively transferring strain.

This relates the macroscopic velocity-gradient to the change in orientation of each crystal. Gillet-Chaulet and others (2005) instead modeled the evolution of the second-order orientation tensor, $\mathbf{a}^{(2)} = \langle \mathbf{c} \otimes \mathbf{c} \rangle$, with an equation derived from Jeffery's equation for a single grain. This has the advantage of only requiring the integration of six independent values. More generally, orientation distribution functions can be decomposed into an orthogonal expansion using orientation tensors $\mathbf{a}^{(n)}$ (with $\mathbf{a}^{(4)} = \langle \mathbf{a} \otimes \mathbf{a} \otimes \mathbf{a} \otimes \mathbf{a} \rangle$ and so on.), similar to a spherical harmonic expansion. In this respect, using the second-order-tensor form of Jeffery's equation is equivalent to a partial expansion of the orientation distribution function up to second order. By evolving each particle separately with Jeffery's equation, this model makes no assumptions about the form of the orientation distribution function, although it is more computationally intensive than closure-based approximations.

Nearest-neighbor stress-transfer

The softness parameter allows strain to be transferred between different grains, depending on the effective strain rate of the grain and its neighbors:

$$\epsilon = \xi \left((1 - \gamma) \epsilon_0 + \gamma \sum_{i=1}^n \frac{A_i \epsilon_i}{\epsilon_0} \right) \quad (3)$$

where ϵ_0 and ϵ_i are the effective shear strain rates of the center grain and grain i , respectively. A_i is the normalized area fraction between the center grain and grain i . ξ is a scaling factor taken over the polycrystal to maintain self-consistency with the bulk velocity gradient. The effective strain rates of each grain depend on the homogenization procedure used. This is explained later.

GRAIN RADIUS EVOLUTION

To track the rheological properties of a polycrystal, it is necessary to know the volume of each grain. Grain boundaries migrate in order to minimize energy from dislocations, grain-boundary energy, and other factors. The assumptions on the interactions between grains are the following: A three-dimensional grain has a surface area proportional to r_i^2 and a volume proportional to r_i^3 , where r_i is the radius of a sphere with the same volume. Then, a polycrystal of grains $\{g_i\}$ with volume $V = \sum_i v_i$ where v_i is the volume of grain i , has surface area $S = \sum s_i/2$. For any three-dimensional shape, $\frac{\alpha}{r} v_i = s_i$, for some constant α . Thus, $S = \beta \sum r_i^2$, for some constant β .

Let g^* be an arbitrary interior grain. This grain has neighbors g_1, \dots, g_m , with radii r_i . The grain has a surface area T . The surface that g^* shares with neighbor n_i is S_i , with surface area s_i . Now, assume that s_i is proportional to the surface area of grain g_i , or equivalently, $s_i = \alpha r_i^2$.

Now, examine the interface between g^* and n_i . Due to grain growth, recrystallization, or other processes, this interface moves with velocity u_i outwardly normal to the surface. Thus, taken over all neighboring grains, $\frac{dV^*}{dt} = \sum_i s_i u_i$. Therefore, if a velocity between two grains can be determined, then this provides a means of determining grain-size evolution based on the properties of a grain and its neighbors.

To implement this for a polycrystal, the less computationally intensive way is to declare that each grain has several neighbors with which to determine the growth rate. To deal with grains disappearing or nucleating, originally the polycrystal is declared to have a number of grains with zero radius. Nucleated grains simply assign a nonzero radius to a formerly zero radius grain, and consumed grains are assigned a zero radius.

GRAIN GROWTH

Normal grain growth is induced by a driving force related to the local curvature at the grain surface.

From Durand and others (2006) $\frac{dr_1}{dt}$, the grain-boundary velocity between two grains due to normal grain growth can be given by

$$\frac{dr_1}{dt} = K \left(\frac{1}{r_1} - \frac{1}{r_2} \right) \quad (4)$$

where K is an Arrhenius factor dependent on temperature, and r_1 and r_2 are the mean curvatures of the two grains. The difficulty in implementing this using the procedure outlined in the previous section is to determine the mean curvature. The

mean curvature of each grain at each point on the shared boundary must be the negative of the other to maintain compatibility. In addition, taken over the entire boundary, the integral of the mean curvature over the boundary of the grain must always be at least 4π . This means that, for example, the grain having negative curvature must “make up” that curvature elsewhere on its boundary. In a physical polycrystal, this imbalance would be accounted for by the boundaries of the polycrystal. However, as a simplification, we take the curvature of the boundary to be the harmonic mean of the curvatures of the two surfaces. This means that the smaller grain will have positive curvature on the boundary, which is a reasonable assumption.

RECRYSTALLIZATION AND POLYGONIZATION

Migration (dynamic) recrystallization is driven primarily by lower-strain-energy grains consuming higher-strain energy grains (Duval and Castelnau, 1995). At least at larger scales (after the initial nucleation), this reduction in strain energy can be incorporated into the driving force of grain boundary migration. A grain neighboring a more highly strained grain will advance into the highly strained grain. This is due to the more highly strained grain having higher dislocation density. The dislocations are annihilated by the advancing boundary.

To determine plastic strain, it is necessary to partition the bulk strain rate between grains. First, the bulk polycrystal stress tensor must be determined. In the coordinate system defined by the c-axis, an individual grain possesses a fourth-order viscosity tensor which can be represented as a diagonal 6×6 matrix in Voigt notation (where multiple elements in the tensor are mapped to the same matrix element by symmetries, Helnwein (2001)). The viscosity of the bulk polycrystal is then taken to be the volume-weighted average of each grain’s viscosity tensor rotated into the macroscopic coordinate system. Then, the bulk stress tensor is found from the product of the viscosity tensor and the strain-rate tensor. The strain rates of individual grains are then determined from the bulk stress tensor and the anisotropic viscosity of the individual grain. Following Azuma and Goto-Azuma (1996), the model calculates the effective stress on each grain, which depends on the bulk stress and the orientation of each grain and its neighbors.

Polygonization is caused by dislocations organizing into dislocation walls in grains experiencing elastic strain (Duval and Castelnau, 1995). Lattice misalignment between the two subgrains increases as more dislocations pile up, eventually splitting the grain into two separate grains misaligned by up to several degrees. We use a similar approach to Thorsteinsson (2002). If the difference of the magnitude of the RSS on the basal plane and the applied stress exceeds a critical value, and the accumulated strain exceeds a critical value, the grain splits into two equal portions. The misorientation is proportional to the dislocation density. The new grain’s orientation is between the original grain, and the closest point of preferred orientation.

MODEL VALIDATION

For a variety of flow situations, the model can reproduce characteristic fabrics such as single maxima, and large girdle fabrics. By incorporating recrystallization, double girdle fabrics and small girdles are produced. This is in qualitative agreement with typical ice-core fabric types. In Figure 1, examples are given of several fabric types produced from different flow scenarios.

We validated the model by forcing it with from the West Antarctic Ice Sheet (WAIS) divide ice core. The flow near the WAIS divide ice-core site is dominated by uniaxial extension, with horizontal shear becoming important near the base. Dynamic recrystallization also occurs near the bed. The fabric in the core is a vertical girdle, which transitions to a vertical single maximum fabric near the bottom of the core. We validated the model by forcing it with data from the WAIS divide ice core, including temperature and a thinning function derived from the WDC06 chronology. This is then compared to thin-section data collected from the core (Donald Voigt, personal communication).

Thin Section Data

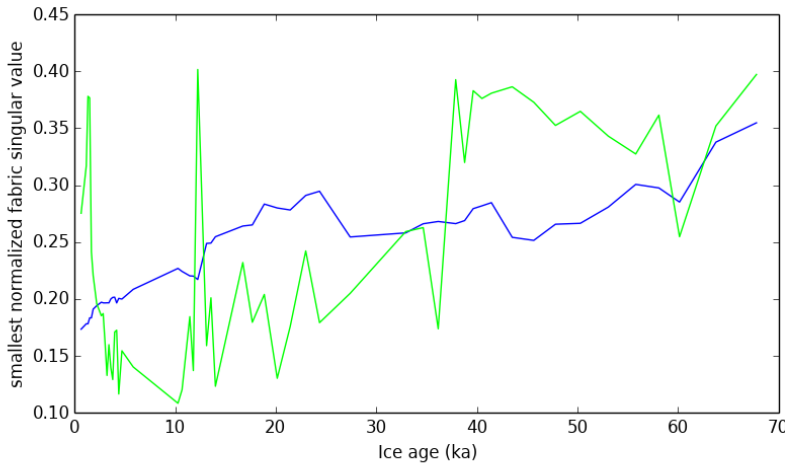
The ice-core thin-section data consist of 54 thin sections from depths of 140 meters to 3405 meters, and a corresponding age range of 480 years to 67,800 B.P. There are several hundred grains in each thin section. The thin-section fabrics display oscillatory behavior. In figure 2, the smallest singular value of each sample is plotted. Some excursions are too large to be explained by sampling error.

The fabric model itself is conceptually a Lagrangian model tracking a single packet of grains as they are advected through the ice sheet over time, whereas each thin section possesses different initial conditions and physical properties. Thus, this is expected to be a significant source of mismatch between observed fabric and modeled fabric. The thin section at 140 m already shows significant development of a preferred orientation. This is consistent with the results of DiPrinzio and others (2005) at Siple Dome, where preferred orientations were observed in the firn as shallow as 22 m. In addition, at the Siple Dome site, recrystallization was found in some layers of shallow, cold ice. A similar process may contribute to the variability observed in the WAIS thin sections.

In addition to likely spatial inhomogeneities, there is sampling error due to small size of fabric samples. From modeling experiments, Thorsteinsson (2002) found that a sample size of around 5000 is needed for a small model variance, whereas the thin sections have sample sizes in the hundreds. However, sampling error is not enough to account for the large differences in fabric seen in the core (see next section).

A common method to summarize a fabric with grain orientations X is to calculate eigenvalues and eigenvectors of the matrix formed by XX^T , or equivalently, calculate the singular values and vectors of the sample matrix. This can capture certain general features such as the strength of a single maximum fabric or a girdle fabric. However, it is unable to capture non-linear features of orientation distributions. For our analysis, we summarize fabrics using the “earth mover distance” (EMD). The EMD between two point sets P_1 and P_2 , with vectors of associated weights for each point W_1 and W_2 , is given by the minimum work required to move the weights from points on P_1 to the points on P_2 . In this case, we are transforming c-axis normal

Fig. 1. Plot of the modeled smallest singular value of the modeled fabric versus that of the WAIS thin-section data. In the upper part of the core, there is a large girdle from extension in one horizontal axis, tending towards a single maximum as simple shear increases.



vectors from one observed fabric to another across the upper hemisphere. The work to move a weight w from a point x to a point y on the upper hemisphere is then given by wd , where d is the great-circle distance. This measure can detect changes in fabric which are not reflected in the fabric eigenvalues, such as the difference between a double girdle and a diffuse single girdle. In addition, it is a relatively robust measure, with qualitatively similar fabrics producing similar results. To model the “girdleness” and single-maximum strength of a fabric, we measure the EMD between the fabric and a perfect single maximum and a perfect girdle. That is, fabrics with c-axis orientations concentrated at only one point, in the case of a single maximum fabric, or along a plane, in the case of a girdle fabric. The results are shown in figure 2.

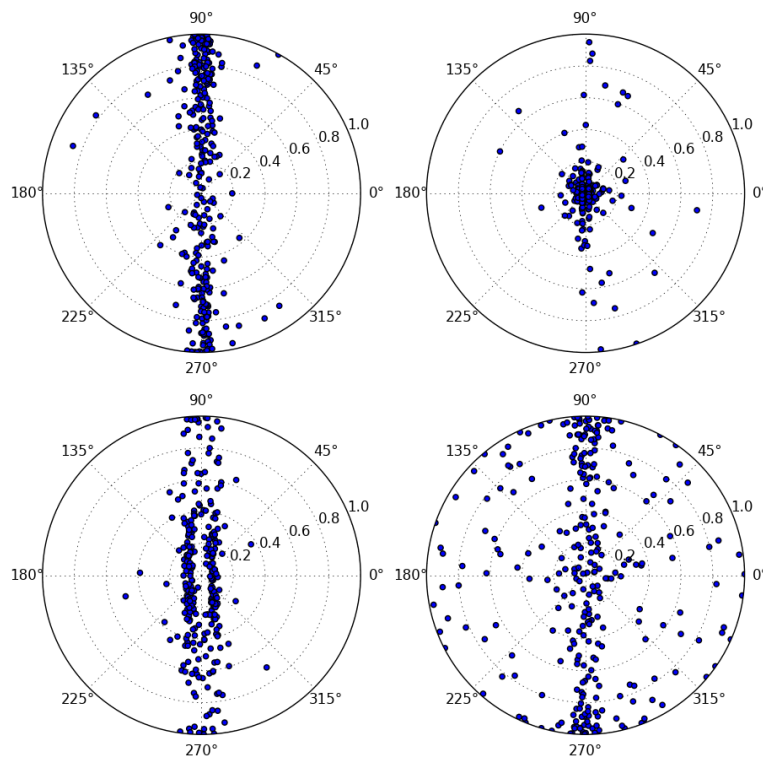
Results

The models can fit the WAIS divide thin-section fabric samples well. Jeffery’s equation does a reasonably good job of predicting the bulk strain rate. The transition from girdle to single maxima deeper in the core due to increased horizontal shear is captured reasonably well, however the thin sections show a more diffuse single maximum developing. This is likely due to the homogeneous strain assumption of the Jeffery’s equation, which overpredicts the strain rate of hard-oriented grains. Using homogeneous stress-derived grain rotation rate with nearest-neighbor interaction provides a better fit, as it is effectively intermediate between homogeneous stress and homogeneous strain assumptions. This is in line with the results of Thorsteinsson (2002) for GRIP thin sections.

For these comparisons, accumulation is assumed to be constant. Varying accumulation may contribute to spurious oscillations of the thinning function used to drive the model. In addition, grain boundary mobility for the model is held constant, which causes recrystallization of Pleistocene ice to be under-predicted. More accurate data representing the past conditions at WAIS would allow for a more accurate fit. However, this does show that the model represents the main features of the core well.

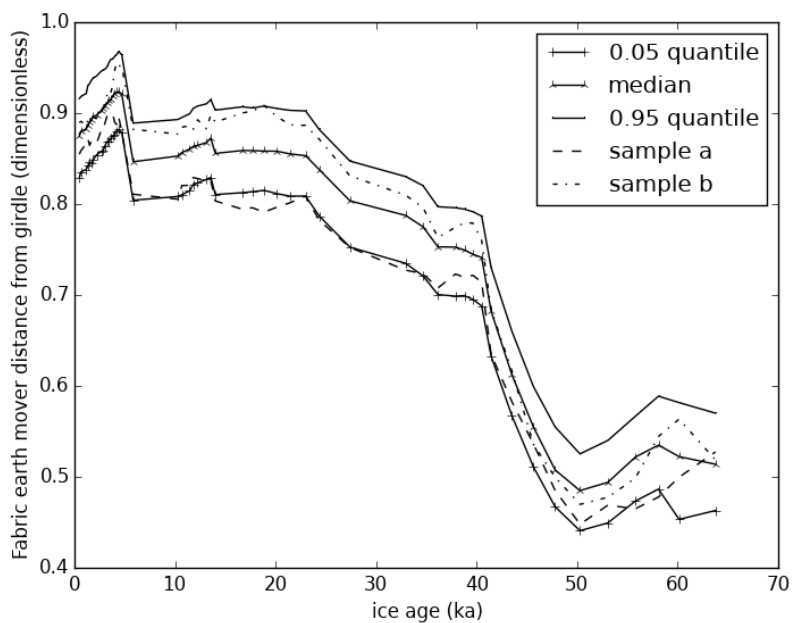
To understand the stochasticity which we may expect, we also repeatedly resampled the c-axis angles of the top thin section at 140m, with replacement, and forced the model with the WAIS divide data with the resampled (bootstrapped) samples as initial conditions. The bootstrapped sample c-axis angles have the same distribution as the original. With 400 grains, the resampled fabrics differ by a fair amount. Variability in EMD between samples stays at roughly the same magnitude throughout the model run. The results (fig 4) show that difference between the 5% and 95% quantiles of girdle EMD of the

Fig. 2. Schmidt plot of fabrics produced under different flow scenarios. (a) Simple shear without recrystallization. (b) Uniaxial extension without recrystallization. (c) Simple shear with recrystallization. (d) Combined simple shear and uniaxial extension.



ensemble stays relatively consistent over time. Thus, initial perturbations of the fabric do not disappear over time. However, the EMDs of the resampled fabrics oscillate over time. The higher frequency oscillations, to a large extent, do not covary between resampled fabrics. A fabric which was previously stronger than another may later become weaker, and vice-versa.

Fig. 3. 90% confidence interval and median of evolution of the distribution of the fabric sample at the top of the core, inferred from repeated bootstrap samples of the thin section data. Two sample realizations are also included.



This is due to both the stochastic of recrystallization, and that nearest neighbors are chosen randomly. Similar behavior can be expected in ice sheets, as the number of nearest neighbors of each grain, and the sizes of the neighbors, can differ greatly from grain to grain. Now, these are limited samples of several hundred grains. Very large fabric samples evolve much more deterministically, as the stochasticity inherent in recrystallization and nearest neighbor selection does not affect bulk properties as much. However, these results do point to significant fabric variability on the meter-scale. This may be important in the development of small-scale flow features like boudinage. In addition, it is possible that the rapidly varying oscillations could cause transient flow on the meter-scale.

!!clarify how different ICs persist over time. Difference between stochastic part and different initial conditions!!

CONCLUSIONS

We showed a fabric evolution model which includes recrystallization and grain rotation. Grain growth and recrystallization depends on nearest-neighbor interactions. The model fits the WAIS ice core fabric data well. The models display a great deal of variability over time, with fabrics oscillating unpredictably over time. This suggests that random fabric variability may be important with small-scale flow. These results show that Jeffery's equation does a reasonably good job of predicting fabric orientation, despite the homogeneous strain assumption. Thus, the orientation-tensor-closure form Jeffery's equation is an appropriate simple model for grain rotation in large-scale flow models (as in Gillet-Chaulet and others (2006)). However, the efficient inclusion of recrystallization and polygonization into flow models is difficult. However, more parameterized treatments may be possible. Folgar and Tucker (1984) developed a version of Jeffery's equation for dilute fiber suspension orientations with rotary diffusion. Such an approach may provide a way forward to treat recrystallization.

Recent results (Montgomery-Smith, 2011) show that coupled Stokes-Jefferys equations modeling fiber suspensions can induce initial perturbations in the orientation distribution function to grow significantly in short amounts of time. The case of ice fabric is extremely similar. This opens up the possibility that small perturbations of the initial fabric could grow into persistent large perturbations. This could be a source of the sometimes chaotic flow disturbances observed in some ice cores. Future work will include coupling of the fabric model to a fully anisotropic ice flow model to examine small-scale features such as boudinage and folding.

References

- Alley, RB, AJ Gow, DA Meese, JJ Fitzpatrick, ED Waddington and JF Bolzan, 1997. Grain-scale processes, folding, and stratigraphic disturbance in the GISP2 ice core, *Journal of Geophysical Research*, **102**(C12), 26819–26.
- Azuma, N., 1994. A flow law for anisotropic ice and its application to ice sheets, *Earth and Planetary Science Letters*, **128**(3–4), 601–614.
- Azuma, Nobuhiko and Kumiko Goto-Azuma, 1996. An anisotropic flow law for ice-sheet ice and its implications, *Annals of Glaciology*, **23**, 202–208.
- Castelnau, O, GR Canova, RA Lebensohn and P Duval, 1997. Modelling viscoplastic behavior of anisotropic polycrystalline ice with a self-consistent approach, *Acta materialia*, **45**(11), 4823–4834.
- DiPrinzio, CL, LA Wilen, RB Alley, JJ Fitzpatrick, MK Spencer and AJ Gow, 2005. Fabric and texture at Siple Dome, Antarctica, *Journal of Glaciology*, **51**(173), 281–290.
- Durand, G, J Weiss, V Lipenkov, JM Barnola, G Krinner, F Parrenin, B Delmonte, C Ritz, P Duval, R Röthlisberger and others, 2006. Effect of impurities on grain growth in cold ice sheets, *Journal of Geophysical Research: Earth Surface* (2003–2012), **111**(F1).
- Duval, P and O Castelnau, 1995. Dynamic recrystallization of ice in polar ice sheets, *Le Journal de Physique IV*, **5**(C3), C3–197.
- Folgar, Francisco and Charles L Tucker, 1984. Orientation behavior of fibers in concentrated suspensions, *Journal of Reinforced Plastics and Composites*, **3**(2), 98–119.
- Gillet-Chaulet, Fabien, Olivier Gagliardini, Jacques Meyssonier, Maurine Montagnat and Olivier Castelnau, 2005. A user-friendly anisotropic flow law for ice-sheet modelling, *Journal of glaciology*, **51**(172), 3–14.
- Gillet-Chaulet, F., O. Gagliardini, J. Meyssonier, T. Zwinger and J. Ruokolainen, 2006. Flow-induced anisotropy in polar ice and related ice-sheet flow modelling, *Journal of Non-Newtonian Fluid Mechanics*, **134**(1), 33–43.
- Gow, Anthony J, 1969. On the rates of growth of grains and crystals in south polar firn, *Journal of Glaciology*, **8**, 241–252.
- Helnwein, Peter, 2001. Some remarks on the compressed matrix representation of symmetric second-order and fourth-order tensors, *Computer methods in applied mechanics and engineering*, **190**(22), 2753–2770.
- Kennedy, Joseph H, Erin C Pettit and Carlos L Di Prinzio, 2013. The evolution of crystal fabric in ice sheets and its link to climate history, *Journal of Glaciology*, **59**(214), 357–373.
- Molinari, A., G.R. Canova and S. Ahzi, 1987. A self consistent approach of the large deformation polycrystal viscoplasticity, *Acta Metallurgica*, **35**(12), 2983 – 2994.
- Montgomery-Smith, Stephen, 2011. Perturbations of the coupled Jeffery-Stokes equations, *Journal of Fluid Mechanics*, **681**, 622–638.
- Pettit, E.C., T. Thorsteinsson, H.P. Jacobson and E.D. Waddington, 2007. The role of crystal fabric in flow near an ice divide, *Journal of Glaciology*, **53**(181), 277–288.
- Sachs, G., 1928. Zur Ableitung einer Fließbedingung, *Z. Vereins Dtsch. Ing.*, **12**(8), 734–736.
- Taylor, Geoffrey Ingram, 1938. Analysis of plastic strain in a cubic crystal, *Stephen Timoshenko 60th Anniversary Volume*, 218–224.

Thorsteinsson, T., 2002. Fabric development with nearest-neighbor interaction and dynamic recrystallization, *J. Geophys. Res.*, **107**(2014), 10–1019.

ALGORITHM FOR THE FABRIC MODEL

Require: Fabric c-axis orientations \mathbf{c}_i , grain radii r_i , bulk strain rate D , vorticity tensor W , connectivity information C_{ij} ;

For each grain \mathbf{g}_i :

-Find local stress on each grain;

-Find areas of each boundary between grains;

For each boundary of grain \mathbf{g}_i

-Find grain growth rate over each boundary due grain boundary energy, dislocation density, and impurity content;

End For

-Add contributions to grain growth of the boundary with each neighbor. Integrate grain growth over each boundary over the timestep;

-Polygonize grain with probability p , depending on strain;

-Rotate grain by integrating Jeffery's equation through the timestep;

End For

-Advance time by δt

-Return to **Start**.